Perovskite and Pyrochlore Modifications of Pb_2MnReO_6: Synthesis, Structure, and Electronic Properties

K. Ramesha,[†] L. Sebastian,[‡] B. Eichhorn,[†] and J. Gopalakrishnan*,[‡]

Department of Chemistry and Biochemistry, Center for Superconductivity Research, University of Maryland, College Park, Maryland 20742, and Solid State and Structural Chemistry Unit, Indian Institute of Science, Bangalore 560012, India

Received July 23, 2002. Revised Manuscript Received November 19, 2002

We describe the synthesis and investigations of Pb_2MnReO_6 in perovskite and pyrochlore modifications. Both the modifications are formed at atmospheric pressure, the perovskite (**I**) at 550 °C and the pyrochlore (**II**) at 600 °C. Rietveld refinements of the structures using the powder XRD data show that oxide **I** adopts the monoclinic ($P2_1/n$) double perovskite structure with partial ordering (∼72%) of Mn^{II}/Re^{VI} at the octahedral sites, while oxide **II** crystallizes in a defect-pyrochlore structure where Mn^{II}/Re^{VI} are disordered at the octahedral sites. The frustrated cation sublattice precludes a long-range ordering of Mn/Re in the pyrochlore structure. **I** is a semiconductor showing evidence for a ferrimagnetic ordering at $T_c \sim 100$ K, but the small saturation magnetic moment ($\langle S \rangle = 0.81$) and the divergence between FC and ZFC magnetization data are consistent with spin-glass-like behavior and a partially ordered Mn/Re in the double perovskite structure. On the other hand, both the Curie−Weiss paramagnetism down to ∼5 K and non-Arrhenius electrical resistivity behavior of **II** suggest a spin-liquid/spin-glass ground state that is consistent with the frustrated cation sublattice of the pyrochlore structure.

Introduction

Double perovskites of the formula A_2MReO_6 (A = Ca, Sr, Ba; M = first row transition metal) have been known for a long time.[1] An early investigation[2] of the A = Ba members, Ba_2MReO_6 using single crystals, revealed that several members of the series (M = Mn, Fe, or Ni) are ferrimagnetic; the M = Fe member is unique in that it is both metallic and ferrimagnetic ($T_c = 334$ K). Similar properties have also been reported for the molybdenum analogues.[3]

A_2MReO_6 and A_2MMoO_6 double perovskites have attracted considerable attention in recent times,[4] following the report of tunneling-type magnetoresistance near room temperature in the A = Sr, M = Fe members.[5,6] The magnetic and magnetoresistive properties of these materials stem from a special electronic structure[5,6] where the itinerant electrons of Re^{5+} ($5d^2$: t_{2g}^2)/Mo^{5+} ($4d^1$: t_{2g}^1) and localized electrons of Fe^{3+} ($3d^5$: $t_{2g}^3e_g^2$) are antiferromagnetically coupled to give rise to a half-metallic ground state with a high degree of spin-polarization at E_F. Although the electronic structure of these materials primarily depends on the electron count in the ordered ($FeReO_6$/$FeMoO_6$) double perovskite array, the influence of the A cation on the structure and properties is clearly seen. Thus, the A = Ca members of both the series, A_2FeReO_6 and A_2FeMoO_6, have a monoclinic (space group $P2_1/n$) ordered perovskite structure,[4b,c] whereas the A = Ba, Sr members have cubic/tetragonal structures. Moreover, the A = Ca member of A_2FeReO_6 is nonmetallic;[4b] interestingly, the ferrimagnetic T_c increases in the order Ca > Sr > Ba.[7]

In an attempt to probe further the influence of the A site cation on the structure and properties of these materials, we have investigated the A = Pb members of A_2MReO_6. Formation of perovskite-type Pb_2MReO_6 for M = Mg, Mn, Fe, Co, and Ni has been known,[8] but no detailed study of structure and properties has been reported. We have chosen lead as the A-site cation

* To whom correspondence should be addressed. E-mail: gopal@sscu.iisc.ernet.in.
[†] University of Maryland.
[‡] Indian Institute of Science.

(1) (a) Sleight, A. W.; Ward, R. *J. Am. Chem. Soc.* **1961**, *83*, 1088. (b) Longo, J. M.; Ward, R. *J. Am. Chem. Soc.* **1961**, *83*, 2816. (c) Sleight, A. W.; Longo, J. M.; Ward, R. *Inorg. Chem.* **1962**, *1*, 245.

(2) Sleight, A. W.; Weiher, J. F. *J. Phys. Chem. Solids* **1972**, *33*, 679.

(3) (a) Patterson, F. K; Moeller, C. W.; Ward, R. *Inorg. Chem.* **1963**, *2*, 196. (b) Nakagawa, T. *J. Phys. Soc. Jpn.* **1968**, *24*, 806. (c) Nakayama, S.; Nakagawa, T.; Nomura, S. *J. Phys. Soc. Jpn.* **1968**, *24*, 219.

(4) (a) Prellier, W.; Smolyaninova, V.; Biswas, A.; Galley, C.; Greene, R. L.; Ramesha, K.; Gopalakrishnan, J. *J. Phys.: Condens. Matter* **2000**, *12*, 965. (b) Gopalakrishnan, J.; Chattopadhyay, A.; Ogale, S. B.; Venkatesan, T.; Greene, R. L.; Millis, A. J.; Ramesha, K.; Hannoyer, B.; Marest, G. *Phys. Rev. B* **2000**, *62*, 9538. (c) Alonso, J. A.; Casais. M. T.; Martínez-Lope, M. J.; Martinez, J. L.; Velasco, P.; Muñoz, A.; Fernández-Diaz, M. T. *Chem. Mater.* **2000**, *12*, 161. (d) Viola, M. C.; Martínez-Lope, M. J.; Alonso, J. A.; Velasco, P.; Martínez, J. L.; Pedregosa, J. C.; Carbonio, R. E.; Fernández-Díaz, M. T. *Chem. Mater.* **2002**, *14*, 812. (e) Yamamota, T.; Liimatainen, J.; Lindén, J.; Karppinen, M.; Yamauchi, H. *J. Mater. Chem.* **2000**, *10*, 2342. (f) Wu, H. *Phys. Rev. B* **2001**, *64*, 125126.

(5) Kobayashi, K.-I.; Kimura, T.; Sawada, H.; Terakura, K.; Tokura, Y.; *Nature* **1998**, *395*, 677.

(6) Kobayashi, K.-I.; Kimura, T.; Tomioka, Y.; Sawada, H.; Terakura, K.; Tokura, Y. *Phys. Rev. B* **1999**, *59*, 11159.

(7) Lofland, S. E.; Scabarozi, T.; Kale, S.; Bhagat, S. M.; Ogale, S. B.; Venkatesan, T.; Greene, R. L.; Gopalakrishan, J.; Ramesha, K. *IEEE Trans. Magn.* **2001**, *37*, 2153.

(8) Gagulin. V. V.; Fadeeva, N. V.; Belous, A. G.; Sevastianova, L. A.; Titov, A. V.; Plotnikova, M. V.; Mitrofanov, K. P.; Zubova, E. V.; Solovev, S. P.; Venevtsev, Yu. N. *Phys. Status Solidi A* **1977**, *44*, 247.

10.1021/cm0207494 CCC: $25.00 © 2003 American Chemical Society
Published on Web 01/04/2003

because Pb^{2+} with its $6s^2$ lone pair is known to influence the structure and properties of AMO_3 oxides.[9] For instance, $PbTiO_3$ has a much higher ferroelectric Curie temperature (T_c = 766 K) than $BaTiO_3$ (T_c = 393 K) that cannot be explained on the basis of ionic radii difference.[9] AMO_3 oxides with lone pair cations such as $PbReO_3$ and $BiRhO_{3+x}$ adopt a pyrochlore structure at ambient pressures instead of the expected perovskite structure.[10,11] Both the oxides however transform to a perovskite structure at high pressures.

Our investigations of Pb_2MReO_6 have revealed that the M = Mn composition is unique, crystallizing in both perovskite and pyrochlore modifications at atmospheric pressure. Unlike the perovskite structure, the pyrochlore structure has a frustrated cation sublattice.[12] Accordingly, stabilization of the same composition (Pb_2MnReO_6) in two different structures provides a rare opportunity to investigate the influence of structure and Mn/Re ordering (or the lack of it) on the electronic properties. Indeed, our results, which are reported herein, reveal significant differences in the electrical and magnetic properties of the two structural modifications of Pb_2MnReO_6.

Experimental Section

Synthesis. Polycrystalline Pb_2MnReO_6 samples were synthesized by a two-step process. First, a precursor oxide of composition $Pb_2ReO_{5.5}$ was prepared by reacting stoichiometric quantities of PbO and Re_2O_7 in flowing Ar at 550 °C for 12 h. Then, the resultant oxide was mixed with required quantities of Mn_2O_3 and Mn according to eq 1 to obtain the stoichiometry Pb_2MnReO_6.

$$Pb_2ReO_{5.5} + {}^1/_6Mn_2O_3 + {}^2/_3Mn \rightarrow Pb_2MnReO_6 \qquad (1)$$

Pellets of the mixture were heated in evacuated sealed tubes. The perovskite phase for Pb_2MnReO_6 was obtained by heating the mixture at 550 °C for a total duration of 24 h with three intermediate grindings. The pyrochlore phase of Pb_2MnReO_6 was obtained by separately heating the reaction mixture at 600 °C for 48 h.

dc resistivity (ρ) was measured between 5 and 300 K, on bars with approximate dimensions of (1 × 2 × 8) mm^3, using the standard four-probe method. Zero-field-cooled (ZFC) and field-cooled (FC) dc magnetic measurements were carried out using a SQUID (MPMS Quantum Design) magnetometer in the same temperature range. Oxygen stoichiometry was determined by a reduction in 1:1 hydrogen/argon using a Cahn TG-131 system.

X-ray Structural Analysis. X-ray powder diffraction (XRD) patterns were recorded using a Bruker C2 Discover X-ray Powder Diffractometer (Cu Kα radiation) with an area detector. XRD patterns were indexed using the MDI program Jade. For refinement, the powder XRD data were collected in the 2θ range 3−100°, in 7 frames with 1800-s exposure time for each frame. Structure refinements were carried out by the Rietveld method using the program FULLPROF.[13] The profiles were fitted with pseudo-Voigt profile functions and profile parameters such as scale factor, three-half-width parameters, zero error, and asymmetry parameters were refined along with unit cell parameters.

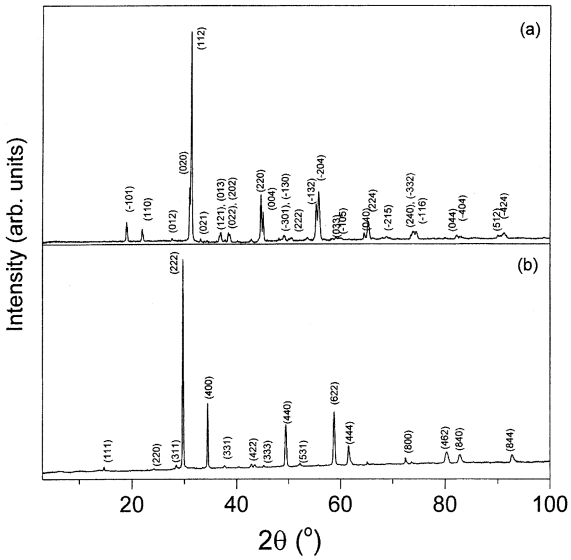

Figure 1. Powder XRD patterns of (a) perovskite and (b) pyrochlore forms of Pb_2MnReO_6.

For the perovskite Pb_2MnReO_6 oxide, refinements were carried out in the ordered double perovskite space group $P2_1/n$ with Ca_2FeMoO_6 as the model structure.[4c] The coordinates for the Pb atom were first refined to convergence followed by oxygen positions with fixed thermal parameters and occupancy for all the atoms. The occupancies of Mn and Re atoms at 2c and 2d sites were then refined together, keeping the overall occupancies for the site fixed at 1.0. Thermal parameters for Mn and Re atoms occupying the same site were linked. Since the refinement gave occupancies of Pb and oxygen atoms as expected, these occupancies were fixed at 1.0 in the final stage of the refinement. We also tried to refine the structure on the space group $I2/m$ but the presence of weak reflections corresponding to 331, 113, and 014 indices ruled out this space group.

For the Pb_2MnReO_6 pyrochlore, the refinement was carried out using space group $Fd3m$ with Pb at 16d, Mn/Re at 16c, and O1 at 48f and O2 at 8b crystallographic positions. The position parameter x of the oxygen atom at the 48f position was refined first (heavy atoms are at special positions in this space group) with a fixed occupancy and thermal parameters for all the atoms. The occupancy for Mn/Re were refined, fixed followed by the refinement of thermal parameters for the sites. Finally, the oxygen occupancies were allowed to refine followed by the thermal parameters. The results show that the O2 site is vacant.

Results and Discussion

General. We could prepare both perovskite and pyrochlore modifications of Pb_2MnReO_6 at atmospheric pressure by varying the synthesis temperature for reaction 1. Essentially, perovskite Pb_2MnReO_6 is a low-temperature phase forming at 550 °C and pyrochlore Pb_2MnReO_6 is a high-temperature phase that forms at 600 °C. The oxygen contents of both the phases, determined by thermogravimetry in H_2/Ar (1:1), correspond exactly to the stoichiometric composition, Pb_2MnReO_6 (weight loss observed for both phases is 10.64 ± 0.01%, and the weight loss expected for the reduction reaction, $Pb_2MnReO_6 + 5H_2 \rightarrow 2Pb + Re + MnO + 5H_2O$ is 10.64%). Laboratory powder XRD patterns (Figure 1) show formation of single-phase perovskite and pyrochlore phases without a detectable impurity. The pattern for perovskite Pb_2MnReO_6 is similar to the patterns of ordered double perovskites[14] and can be indexed on

(9) Cohen, R. E. *Nature* **1992**, *358*, 136.
(10) Longo, J. M.; Raccah, P. M.; Goodenough, J. B. *Mater. Res. Bull.* **1969**, *4*, 191.
(11) (a) Longo, J. M.; Raccah, P. M.; Kafalas, J. A.; Pierce, J. W. *Mater. Res. Bull.* **1972**, *7*, 137. (b) Kafalas, J. A.; Longo, J. M. *Mater. Res. Bull.* **1970**, *5*, 193.
(12) Greedan, J. E. *J. Mater. Chem.* **2001**, *11*, 37.
(13) Rodriguez-Carvajal, J. *Physica B (Amsterdam)* **1993**, *192*, 55.

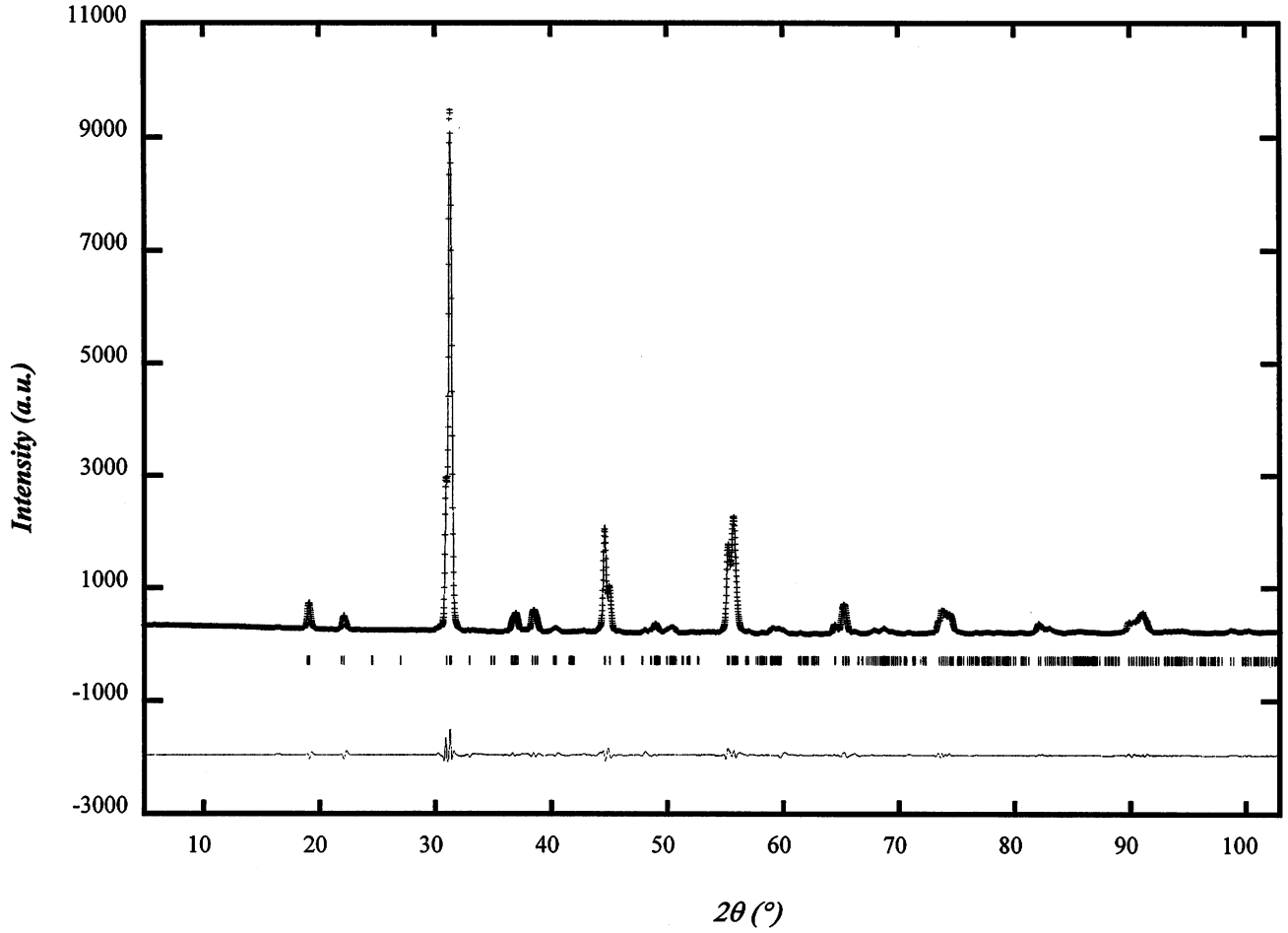

Figure 2. Observed (+), calculated (−), and difference (bottom) Rietveld refined powder XRD profiles of perovskite Pb_2MnReO_6.

a monoclinic cell, space group $P2_1/n$, with $a = 5.702(1)$ Å, $b = 5.769(1)$ Å, $c = 8.042(1)$ Å, and $\beta = 90.09°$. The pattern of pyrochlore Pb_2MnReO_6 is typical of defect pyrochlores[10,11] and can be indexed on a cubic cell, space group $Fd3m$, with $a = 10.412$ Å.

Perovskite Pb_2MnReO_6. We have refined the structure of perovskite Pb_2MnReO_6 from powder XRD data using the model of Ca_2FeMoO_6[4c] in the space group $P2_1/n$. Observed, calculated, and difference profiles are shown in Figure 2 and the crystallographic data obtained from the refinement are given in Table 1. We see that the structure (Figure 3) of perovskite Pb_2MnReO_6 is similar to that of ordered (monoclinic) double perovskites with a rock-salt-type of ordering of Mn/Re ordering[14] at the octahedral (2c and 2d) sites. The ordering however is partial (~72%) corresponding to 0.86/0.14 occupancy (Table 1). The incomplete ordering is likely due to the low temperature of synthesis (550 °C). It must be mentioned that the structure described here for the perovskite Pb_2MnReO_6 would at best be an average structure, considering that several Pb(II)-containing double perovskites such as Pb_2CoWO_6 and Pb_2MgWO_6 possess complex incommensurate structures.[15] The complexity of the structures arises from displacement of the lone pair Pb(II) and the consequent oxygen disorder, even as the octahedral-site cations are perfectly ordered. We therefore believe that the structure of Pb_2MnReO_6 perovskite would also be more complex than what is described here; a neutron diffraction study is essential for determining the details of the structure including the positions of oxygen atoms. In view of the likely uncertainty in the oxygen atom positions, the average M(1)−O and M(2)−O bond distances, 2.144 and 1.996 Å, obtained from the present refinement (Table 1) should be regarded as reasonable values; the corresponding values calculated as weighted sum of ionic radii for the M(1)/M(2) site occupancies are 2.140 and 1.939 Å.

Magnetic and electrical properties are consistent with the partially ordered double-perovskite structure of Pb_2MnReO_6. It is a semiconductor ($\rho_{300} \sim 10^2$ Ω-cm) with a temperature variation that is nearly Arrhenius-like ($E_a = 0.13$ eV) (Figure 4). Magnetic susceptibility data (Figure 5a) show a clear indication for a ferrimagnetic ordering with $T_c \sim 100$ K. The plot of M vs H (Figure 5b) shows that the moment does not saturate but approaches a value of 14.9 emu/g corresponding to $\langle S \rangle = 1$ where

$$M = N/\mathrm{MW} \times \mathrm{g} \times \mu_B \langle S \rangle$$

This observed moment (12.01 emu/g) is much smaller than the expected value of 29.72 emu/g ($\langle S \rangle = 2$) for a ferrimagnetic ordering of high-spin Mn^{2+} ($3d^5 : t_{2g}^3 e_g^2$)

(14) Anderson, M. T.; Greenwood, K. B.; Taylor, G. A.; Poeppelmeier, K. R. *Prog. Solid State Chem.* **1993**, *22*, 197.

(15) (a) Baldinozzi, G.; Calvarin, G.; Sciau, Ph.; Grebille, D.; Suard, E. *Acta Crystallogr., Sect. B: Struct. Sci.* **2000**, *56*, 570. (b) Baldinozzi, G.; Sciau, Ph.; Pinot M.; Grebille, D. *Acta Crystallogr., Sect. B: Struct. Sci.* **1995**, *51*, 668.

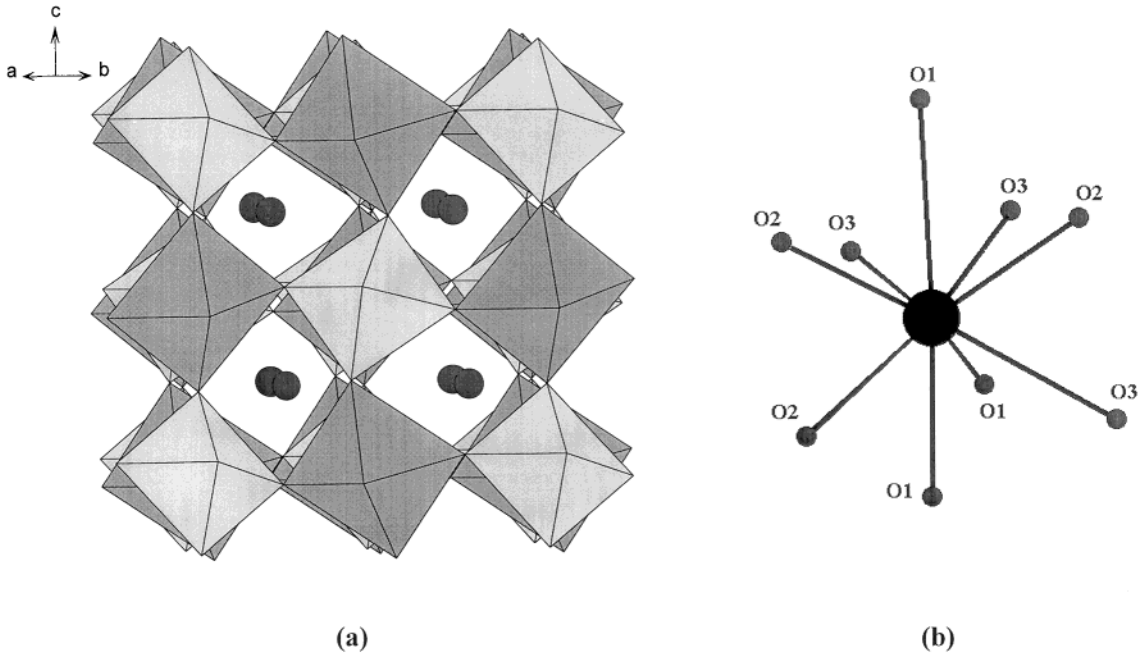

Figure 3. Crystal structure of perovskite Pb_2MnReO_6 (a). The coordination polyhedron around Pb^{II} is shown in (b).

Table 1. Crystallographic Data for Perovskite Pb_2MnReO_6 Together with Selected Bond Lengths and Bond Angles

atom	site	*x*	*y*	*z*	*B* (Å^2)	occupancy
Pb	4e	0.9743	0.0126	0.2458	0.85(4)	1.00
Mn1	2c	0.5	0	0.5	0.31(1)	0.86(1)
Re1	2c	0.5	0	0.5	0.31(1)	0.14(1)
Re2	2d	0.5	0	0	0.42(2)	0.86(1)
Mn2	2d	0.5	0	0	0.42(2)	0.14(1)
O1	4e	0.0623(1)	0.4452(2)	0.2612(1)	1.00	1.00
O2	4e	0.7002(1)	0.2833(3)	0.0382(1)	1.00	1.00
O3	4e	0.2293(2)	0.2118(2)	0.9621(2)	1.00	1.00

cell parameters:
$a = 5.7054(1)$ Å, $b = 5.7714(1)$ Å, $c = 8.0415(1)$ Å, $\beta = 90.14(1)°$
reliability factors:
$R_p = 5.31\%$, $R_{wp} = 7.53\%$, $R_{Bragg} = 5.96\%$, $R_F = 5.21\%$, $\chi^2 = 1.83$

Selected Bond Distances (Å) and Angles (deg)

$M(1)O_6$ Octahedra
M(1)−O1 (×2) = 2.153(4)
M(1)−O2 (×2) = 2.142(3)
M(1)−O3 (×2) = 2.138(2)
⟨M(1)−O⟩ = 2.144(3)

$M(2)O_6$ Octahedra
M(2)−O1 (×2) = 1.979(4)
M(2)−O2 (×2) = 1.993(3)
M(2)−O3 (×2) = 2.018(2)
⟨M(2)−O⟩ = 1.996(3)
M(1)−O1−M(2) (×2) = 153.32(4)
M(1)−O2−M(2) (×2) = 154.61(4)
M(1)−O3−M(2) (×2) = 158.38(6)

PbO_9 Polyhedra
Pb−O1 = 2.550(1)
Pb−O1 = 2.673(1)
Pb−O1 = 3.087(1)
Pb−O2 = 2.402(8)
Pb−O2 = 2.768(10)
Pb−O2 = 2.926(11)
Pb−O3 = 2.411(8)
Pb−O3 = 2.943(12)
Pb−O3 = 2.742(9)

and Re^{6+} ($5d^1$: t_{2g}^1) in Pb_2MnReO_6 and contrasts the observed saturation moment of $\sim\langle S\rangle = 2$ with $T \sim 100$ K reported[2,16] for ordered Ba_2MnReO_6. Although the observed saturation moment in Pb_2MnReO_6 is close to

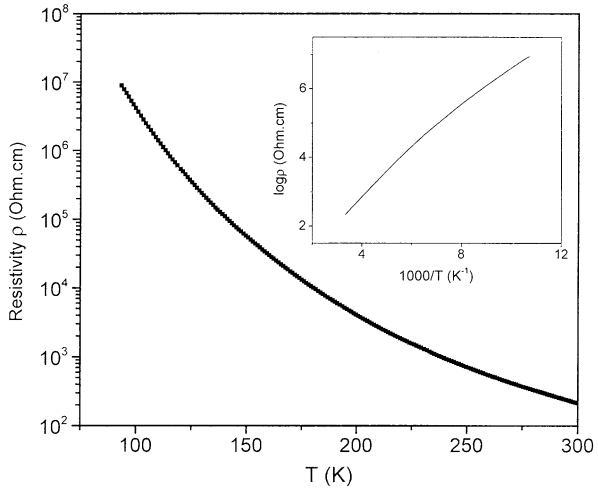

Figure 4. Electrical resistivity (ρ) vs temperature (T) plot for perovskite Pb_2MnReO_6. Inset shows the corresponding log ρ vs ($1/T$) plot.

that expected for a ferrimagnetic Mn^{3+} ($3d^4$: $t_{2g}^3e_g^1$)/Re^{5+} ($5d^1$: t_{2g}^2) double perovskite, we attribute the smaller than expected moment to the incomplete ordering of the Mn^{2+}/Re^{5+} ions in the Pb_2MnReO_6 structure. The small saturation moment together with a divergence of ZFC and FC magnetization and the semiconducting behavior are all in agreement with the partially ordered double perovskite structure for Pb_2MnReO_6. Although the compound is paramagnetic above 100 K, the plot of χ_M^{-1} vs T is not linear throughout the temperature region 100−300 K. Attempted fits of the data in the temperature range 100−300 K to the Curie−Weiss law, with a correction for temperature-independent paramagnetism (TIP), $\chi_M = \chi_0 + C/(T - \theta)$ gave $\chi_0 = 5.8 \times 10^{-3}$ emu/mol, $C = 1.55$, which are both unrealistic. The spin-only moment (5.4 μ_B) calculated from a Curie−Weiss fit $\chi_M = C/(T - \theta)$ above 200 K is

(16) Khattak, C. P.; Cox, D. E.; Wang, F. F. Y. *J. Solid State Chem.* **1975**, *13*, 77.

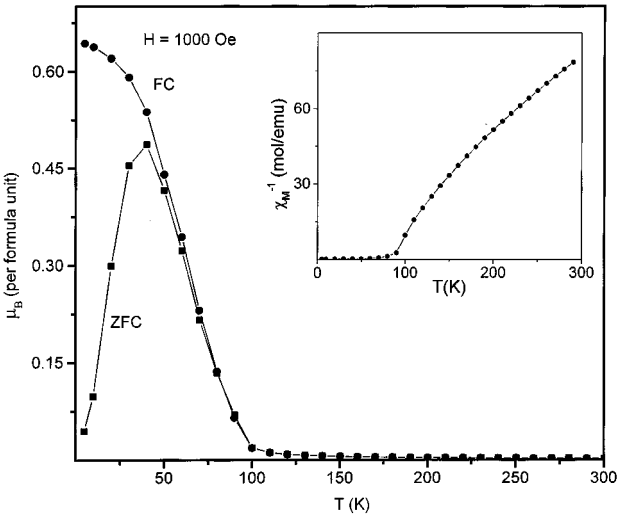

Figure 5. Magnetic susceptibility data for perovskite Pb_2MnReO_6. Inset shows the corresponding χ_M^{-1} vs T plot.

Table 2. Crystallographic Data for Pyrochlore Pb_2MnReO_6 Together with Selected Bond Lengths and Bond Angles

atom	site	x	y	z	B (Å^2)	occupancy
Pb	16d	0.5	0.5	0.5	0.34	1.00
Mn/Re	16c	0	0	0	0.23	1.00
O1	48f	0.3291(1)	0.1250	0.1250	0.63	1.00

cell parameter: $a = 10.412$ (1) Å

reliability factors:

$R_p = 8.1\%$, $R_{wp} = 8.9\%$, $R_{Bragg} = 8.1\%$, $R_F = 7.8\%$, $\chi^2 = 2.1$

Bond Distances (Å) and Angles (deg) for Pb_2MnReO_6

Mn/ReO_6 Octahedra

Mn/Re−O1 (×6) = 2.016(2)

Mn/Re−O1−Mn/Re = 96.32(1), 83.68(1)

O1−Mn/Re−O1 = 131.84(1)

PbO_6 Polyhedra

Pb−O1 (×6) = 2.561(1)

slightly smaller than the expected magnetic moment (6.2 μ_B) for noninteracting Mn^{2+}/Re^{6+}paramagnetic array. We attribute the low moment to short-range magnetic correlations that become more pronounced closer to T_c.

Pyrochlore Pb_2MnReO_6. We have refined the crystal structure of pyrochlore Pb_2MnReO_6 from powder XRD data in the $Fd3m$ space group using the model of defect pyrochlores[10,11] containing Bi^{3+}/Pb^{2+}. Observed, calculated, and difference profiles are shown in Figure 6 and the crystallographic data derived from the refinement are given in Table 2. The structure is drawn in Figure 7. From the structure refinement, we see that the Mn/Re atoms are disordered at 16c sites, the O1 oxygen site (48f) is fully occupied, and the O2 oxygen site (8b) is empty, as expected for a typical defect pyrochlore structure with AMO_3 stoichiometry.[10,11] The data are also consistent with the O_6 oxygen stoichiometry obtained from the TG analysis for the pyrochlore Pb_2MnReO_6. For AMO_{3+x} defect pyrochlores in general, the O1 (48f) sites are fully occupied, giving the octahedral M_2O_6 framework and the O2 (8b) sites are empty ($x = 0$) or partially occupied ($x > 0$). The positional parameter for O1 ($x = 0.329$) is within the range ($0.305 \leq x \leq 0.355$) reported[11a] for pyrochlores in general. The $(Mn/Re)O_6$ octahedron is nearly regular with a Mn/Re−O distance of 2.02 Å, reflecting the statistical distribution of Mn/Re atoms at the octahedral (16c) sites (Mn^{II}/Re^{VI}−O distance expected on the basis of average octahedral radii is 2.09 Å). The Pb−O coordination and Pb−O bond distances are similar to other defect pyrochlores[17] containing Pb^{II}. Moreover, a bond valence analysis of Pb in pyrochlore Pb_2MnReO_6 gives a valence of +1.78.

Formation of Pb_2MnReO_6 in the defect pyrochlore structure is a clear manifestation of the influence of the Pb^{II} : $6s^2$ lone pair on the structure. Stabilization of a defect pryochlore structure instead of a perovskite structure for several AMO_{3+x} oxides where A is a lone pair cation ($Bi^{III}/Pb^{II}/Tl^{I}$) at atmospheric pressure has been explained by Longo et al.[10] as arising from a polarization of the $6s^2$ lone pairs of A-site cations by the (8b) oxygen vacancy that results in the formation of a trap-mediated A−A bond. When this A−A bond energy is greater than the loss in Madelung energy, a pyrochlore structure is stablized instead of a perovskite structure. Alternately, it could be due to the preference of oxygen for a tetrahedral coordination of metal atoms (pyrochlore structure) instead of a 6-fold coordination (4A + 2M) in the perovskite structure, when both A and M atoms are not highly electropositive, as pointed out by Sleight.[18]

Since the pyrochlore structure is less dense than the perovskite structure for a given AMO_3 composition, the pyrochlore phase is obtained at atmospheric pressure and it transforms to the perovskite phase at high pressures[11] for several AMO_{3+x} oxides where A = Pb^{II}/Bi^{III}. For Pb_2MnReO_6 described here also, we see that the pyrochlore phase is less dense than the perovskite phase (volume per formula unit are 141.01 and 132.04 Å^3 respectively for the pyrochlore and perovskite phases), but what is remarkable is that we are able to synthesize both the phases at atmospheric pressure by a slight variation in synthesis temperature (550 °C for perovskite and 600 °C for pyrochlore). Another major difference is that while the perovskite structure permits a long-range ordering of M site cations to give ordered double perovskites[14] for $A_2MM'O_6$ compositions, the pyrochlore structure containing a "frustrated" cation sublattice (Figure 7) precludes a long-range ordering of octahedral site cations.[12] Accordingly, we do not find evidence for an ordering of Mn/Re atoms in the pyrochlore structure of Pb_2MnReO_6. The absence of long-range ordering has a significant influence in the electrical and magnetic properties of pyrochlore Pb_2MnReO_6 vis-à-vis those of perovskite Pb_2MnReO_6.

The magnetic susceptibility behavior (Figure 8) is clearly Curie−Weiss with no indication of magnetic ordering down to ~5 K, although the negative (−40 K) suggests short-range antiferromagnetic correlations. The magnetic moment (7.4 μ_B) obtained from the χ_M^{-1} vs T plot is slightly higher than the spin-only moment expected for Mn^{2+}/Re^{6+} (6.2 μ_B). The higher μ_B could be due to short-range antiferromagnetic correlations between Mn^{2+} and Re^{6+}, which would give rise a net magnetic moment that is larger than the value expected for a noninteracting paramagnetic array of Mn^{2+}/Re^{6+}.

(17) Abakumov, A. M.; Shpanchenko, R. V.; Antipov, E. V.; Kopnin, E. M.; Capponi, J. J.; Marezio, M.; Lebedev, O. I.; Van Tendeloo, G.; Amelinckx, S. *J. Solid State Chem.* **1998**, *138*, 220.

(18) Sleight, A. W. *Mater. Res. Bull.* **1969**, *4*, 377.

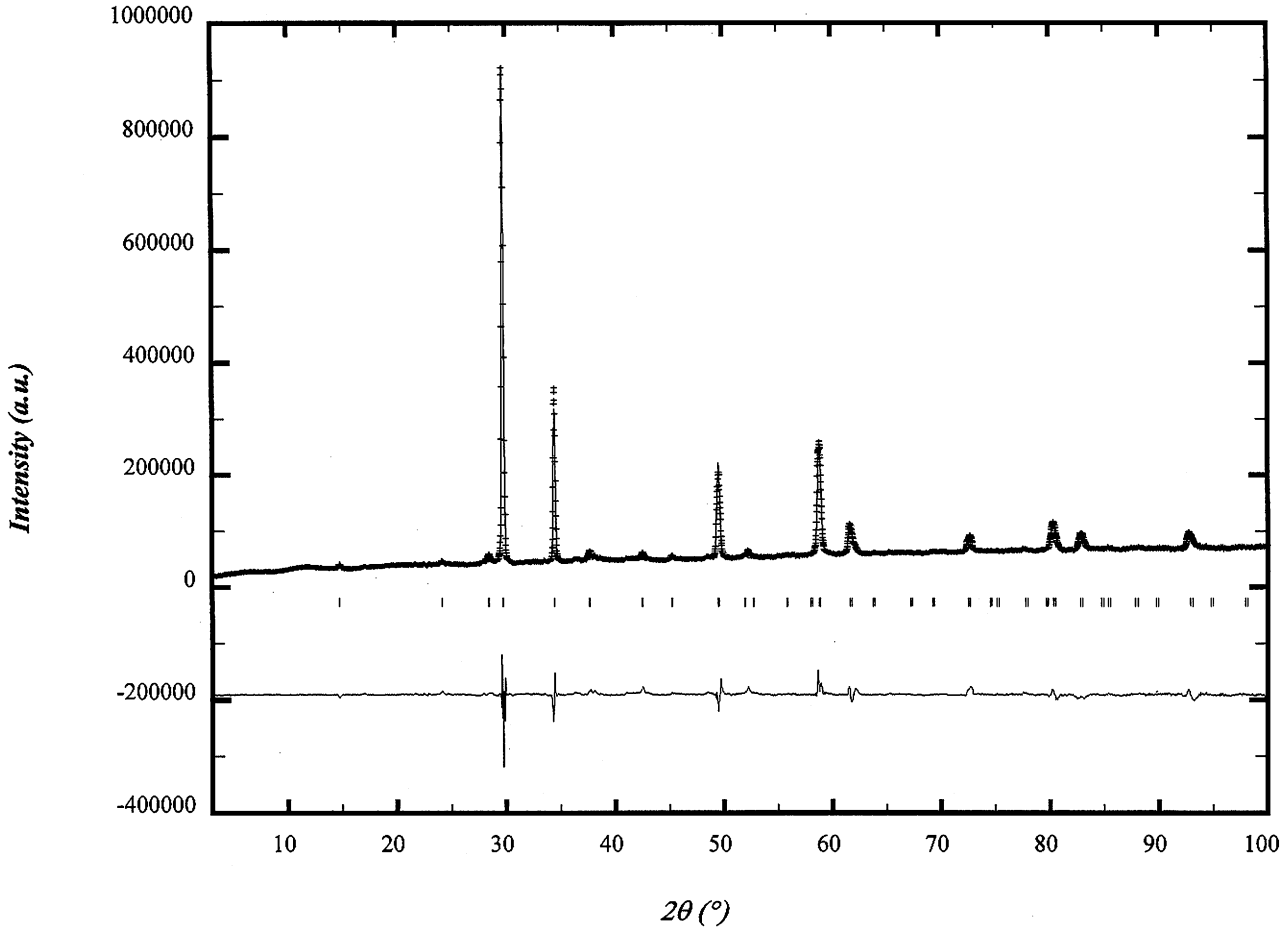

Figure 6. Observed (+), calculated (−), and difference (bottom) Rietveld refined powder XRD profiles of pyrochlore Pb_2MnReO_6.

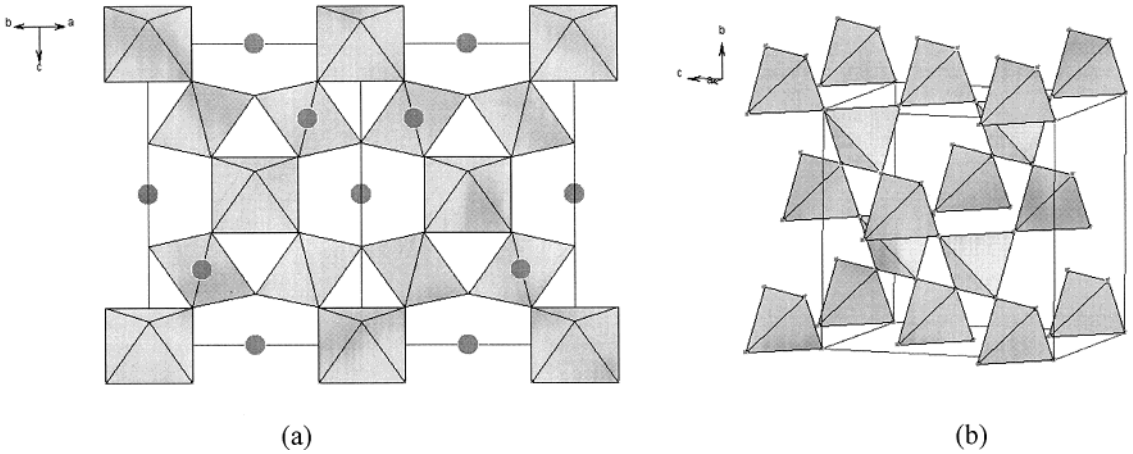

Figure 7. Crystal structure of pyrochlore Pb_2MnReO_6 showing the octahedral network (a). The Mn/Re cation sublattice at 16c positions is shown in (b).

One would have expected the absence of long-range ordering of Mn^{2+}/Re^{6+} in the frustrated cation sublattice of pyrochlore Pb_2MnReO_6 to give rise to spin-glass behavior similar to, for example, that of $Y_2Mo_2O_7$.[12] Pyrochlore $Y_2Mo_2O_7$ is a well-ordered crystalline solid and is an insulator with no long-range magnetic order down to 4.2 K, but shows typical spin-glass behavior in its magnetic and other properties;[12,19] the characteristic divergence between FC and ZFC susceptibilities shows that spin-freezing occurs at 22 K. The absence of such a spin-glass freezing with Curie−Weiss behavior of susceptibility down to 5 K for pyrochlore Pb_2MnReO_6 (Figure 8) appears unique among the geometrically frustrated pyrochlore oxides, suggesting that the behavior is more like a spin-liquid rather than spin-glass.[12] The fact that the isocompositional Pb_2MnReO_6 perovskite shows strong magnetic correlations supports this proposal. The electrical resistivity data (Figure 9) also support the spin-liquid/spin-glass model for pyrochlore Pb_2MnReO_6. The resistivity of the material is rather low ($\rho \sim 0.5$ Ω-cm at 300 K) that remains essentially constant down to ~50 K; thereafter, it shows

(19) Greedan, J. E.; Sato, M.; Yan Xu.; Razavi, F. S. *Solid State Commun.* **1986**, *59*, 895.

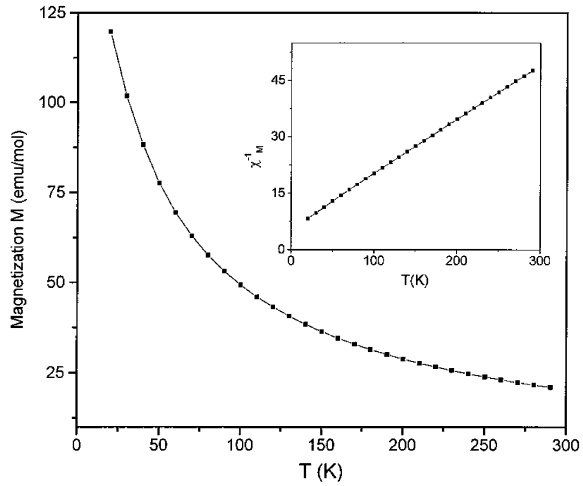

Figure 8. Magnetic susceptibility data for pyrochlore Pb_2MnReO_6. Inset shows the corresponding χ_M^{-1} vs T plot.

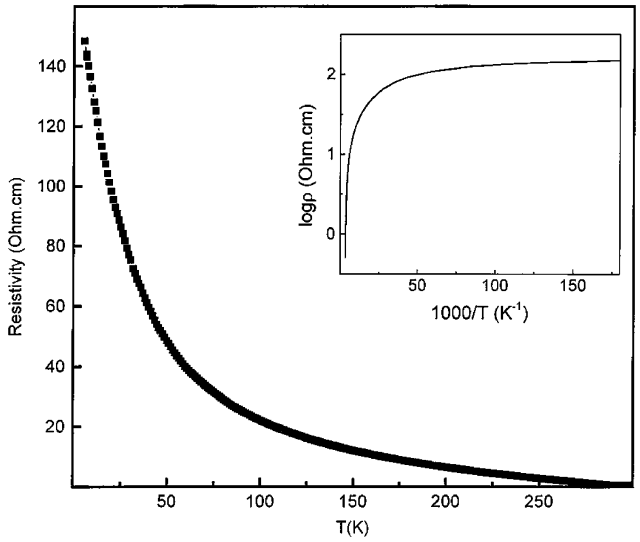

Figure 9. Electrical resistivity (ρ) vs temperature (T) plot for pyrochlore Pb_2MnReO_6. Inset shows the corresponding log ρ vs $1/T$ plot.

a sharp increase, giving essentially a non-Arrhenius temperature dependence that is somewhat similar to that of semiconducting $R_2Mo_2O_7$ pyrochlores.[20] Further studies at low temperatures ($T < 20$ K) are essential for establishing the electronic ground state of pyrochlore Pb_2MnReO_6. Pressure-induced transformations of pyrochlore Pb_2MnReO_6 to the perovskite structure would also be of interest to investigate because the perovskite Pb_2MnReO_6 obtained under pressure would likely have a fully ordered Mn/Re sublattice and consequently possess interesting electronic properties.

(20) Ali, N.; Hill, M. P.; Labroo, S.; Greedan, J. E. *J. Solid State Chem.* **1989**, *83*, 178.

Conclusions

We have been able to prepare both perovskite and pyrochlore modifications of the oxide Pb_2MnReO_6 at atmospheric pressure for the first time. Usually, AMO_3 oxides containing $6s^2$ lone pair cations, Pb^{II}/Bi^{III}, adopt a pyrochlore structure at atmospheric pressure, which transforms to a perovskite structure at high pressures. Perovskite Pb_2MnReO_6 crystallizes in the monoclinic double perovskite structure with rock-salt-type of ordering of Mn/Re at the octahedral sites, but the ordering is only partial (~72%), as revealed by Rietveld refinement of powder XRD data. The electrical and magnetic properties are consistent with the partially ordered double perovskite structure of Pb_2MnReO_6. The structure of the pyrochlore modification of Pb_2MnReO_6 is similar to the defect pyrochlore structures of AMO_3 oxides containing Pb^{II}/Bi^{III} at the A site, forming a $MnReO_6$ framework of corner-shared octahedra. The frustrated cation sublattice of the pyrochlore structure however precludes a long-range ordering of Mn/Re at the octahedral sites, giving rise to interesting magnetic and electrical properties. A Curie−Weiss magnetic susceptibility with no evidence for magnetic ordering down to 5 K and a non-Arrhenius electrical resistivity of this material appear to be the consequence of the geometrically frustrated Mn/Re sublattice and likely suggest a spin-liquid electronic ground state that does not seem to freeze into a spin-glass state even at ~5 K in pyrochlore Pb_2MnReO_6.

Acknowledgment. We thank the NSF (DMR-0076460) for support of this work. The work at Bangalore is supported by the Council of Scientific and Industrial Research (CSIR), New Delhi. L.S. thanks the CSIR for the award of a research fellowship. We are grateful to Dr. Serpil Gönen for help with the susceptibility measurements and for valuable discussions.

Supporting Information Available: Calculated and observed powder XRD peak positions for perovskite and pyrochlore Pb_2MnReO_6 (PDF). This material is available free of charge via the Internet at http://pubs.acs.org.

CM0207494